Journal of Optoelectronics and Advanced Materials Vol. 7, No. 2, April 2005, p. 727 - 732

STRUCTURAL AND ELECTRICAL PROPERTIES OF ANTIMONY TRISULFIDE THIN FILMS

N. Tigau*, G. I. Rusu[a], V. Ciupina[b], G. Prodan[b], E. Vasile[c]

Faculty of Science, "Dunarea de Jos" University, Galati, R-6200, Romania
[a]Faculty of Physics, "Alexandru Ioan Cuza" University, Iasi, R-6600, Romania
[b]"Ovidius" University, Constanta, R-8700, Romania
[c]S.C. METAV S.A., Bucuresti, R-7200, Romania

Antimony trisulfide (Sb_2S_3) thin films were deposited onto glass substrates by thermal vacuum evaporation. The film structure was studied by X-ray diffraction (XRD) technique, transmission electron microscopy (TEM) and scanning electron microscopy (SEM). The films deposited at substrate temperature, T_s=300 K, are amorphous. The films with stable polycrystalline structure can be obtained if subjected, after deposition, to a heat treatment, consisting of several heating/cooling cycles. The sequence of grain growth was found to begin with lognormal grain size distribution. The mechanism of electrical conduction is discussed in terms of Seto`s model for polycrystalline semiconducting films. The values of thermal activation energy of electrical conduction have been determined from the $ln\sigma = f(10^3 / T)$ curves.

(Received August 18, 2004; accepted March 23, 2005)

Keywords: Antimony trisulfide, Structural properties, Electrical conductivity

1. Introduction

Antimony trisulfide (Sb_2S_3) attracted the interest of researchers due to their application in the electronic devices, especially in photoconductive target material in television cameras, microwave devices, switching devices and various optoelectronic devices [1-6]. The use the Sb_2S_3 thin films in Schottky barrier solar cells of Pt- Sb_2S_3 and n-Sb_2S_3/p-Ge structures with conversion efficiencies of 5.5 and 7.3 % respectively, has been reported [7,8].

In the last years, a variety of methods have been employed for the growth of high-quality Sb_2S_3 thin films, such as chemical bath deposition in non-aqueous [9] and aqueous media [7,10,11], spray pyrolysis [12,13], flash evaporation [14] and vacuum evaporation [15-18]

The determination of the electronic parameters of semiconducting thin films is essential in testing their suitability. The basic requirements of a good thin film photoelectrode are low resistivity and a large grain size. The large grain size leads to the reduction of the grain boundary area of thin films with important consequences on efficient energy conversion [19]. The low resistivity of photoelectrode is required to minimize the series resistance of the cell [20].

In a series of previous papers [21,22], we have studied some structural and optical properties of Sb_2S_3 thin films prepared by thermal vacuum evaporation technique. In this paper we extended these investigations by studying the temperature dependence of the electrical conductivity on the film thickness and post-deposition heat treatment. The temperature dependence of the electrical conductivity in Sb_2S_3 thin films is explained using a model proposed by Seto [23-26].

* Corresponding author: ntigau@ugal.ro

2. Experimental

Sb_2S_3 thin films were prepared by direct thermal evaporation of fine-grained powder from a quartz crucible with a deposition rate of 2 nms^{-1} onto optically flat precleaned glass substrates, using a coating unit. The vacuum pressure was maintained at 10^{-5} Torr and the substrates were rotated during the deposition process. The source temperature was kept constant 850 K and the source to substrate distance was 8 cm. The substrate temperature was maintained at 300 K during the deposition. After deposition, the films thickness was determined by an interferometric method [27] and for investigated samples ranged between 0.45 and 2.35 μm. The films structure was examined by X-ray diffraction (XRD) technique and transmission electron microscopy (TEM). The surface morphology of the films was examined using a Philips SEM 515 scanning electron microscope, operated at 30 kV.

The electrical conductivity measurements were carried out using aluminium electrodes that form ohmic contact with Sb_2S_3 [16] and deposited by thermal evaporation under vacuum of 10^{-5} Torr before the deposition of Sb_2S_3 films. In all experiments the electrodes were speared by a gap of about 3 mm and width of each electrode was 10 mm. The area defined was 0.3 cm^2. Resistivity of the samples was measured by a d.c. two point probe method in the temperature range 287 K-487 K, using a 6517 A Keithley electrometer. The applied electric fields have intensities ($E<10^2$ Vcm^{-1}). The experimental arrangements used for the study of temperature dependence of electrical conductivity were similar to those described in Ref. [28].

3. Results and discussion

The crystallinity of Sb_2S_3 films was investigated with the XRD [21,22] and electron diffraction measurements. As-deposition Sb_2S_3 thin films shown an amorphous structure but after annealing become polycrystalline. The electron diffraction patterns of Sb_2S_3 thin films, before and after heat treatment at 447 K are given in Fig. 1(a) and (1b). The diffraction rings can be indexed to an orthorhombic structure. The observed values of interplanar spacing, $d_{hk\ell}$, are inserted in electron diffraction pattern in Fig. 1(b). The calculated parameters corresponding to orthorhombic system are a=11.126 Å, b=11.305 Å and c=3.891 Å. The results are in good agreement with the standard PDF card and the previously reported data for Sb_2S_3 [11,29,30].

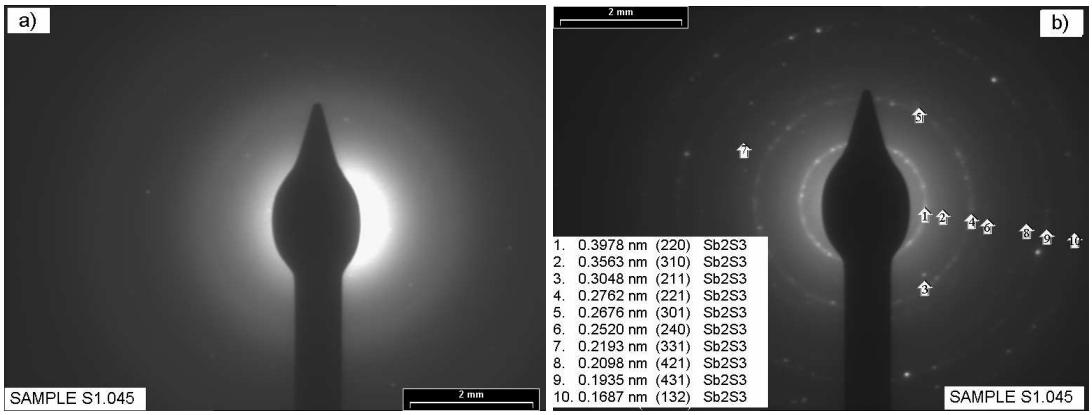

Fig. 1. Electron diffraction patterns of Sb_2S_3 thin films: (a) as-deposited (b) annealed.

The SEM micrographs of investigated samples after heat treatment are shown in Fig. 2. It is clear from the SEM images that the heat treatment leads to completely crystallized grains. The Sb_2S_3 thin films exhibit a grain-like surface morphology.

The crystallite size increases with increasing film thickness. The average size, ℓ, of the Sb_2S_3 crystallites have been calculated from the intercept method [31]:

$$\ell = \frac{k\,L}{N\,m} \tag{1}$$

where L is the line length on the micrograph, N is the number of grains crossed by the line, m is the micrograph magnification (10000×) and k=1 is the shape parameter, assuming spherical grains [31].

Grain size measurements were made on the basis of SEM images. The histograms grain size distribution is shown in Fig. 3(a) and (3b). The line from inserted figures is the best fit lognormal function [32,33]

$$f(D) = \frac{1}{\beta D\sqrt{2\pi}}\,exp\left[-\frac{(\ln D - \ln D_m)^2}{2\beta^2}\right] \tag{2}$$

where the two fitting parameters are D_m, witch equals the mean grain size and β, witch is the standard deviation of $\ln D$.

For all the samples, the fitted lognormal distribution is in good agreement with the histogram distribution in the whole grain size range. The mean grain size, D_m, and standard deviation, β, determined from this method is presented in Table 1. The mean grain size was found to increase from 74 nm to 152 nm when the film thickness increases from 0.45 μm to 2.35 μm.

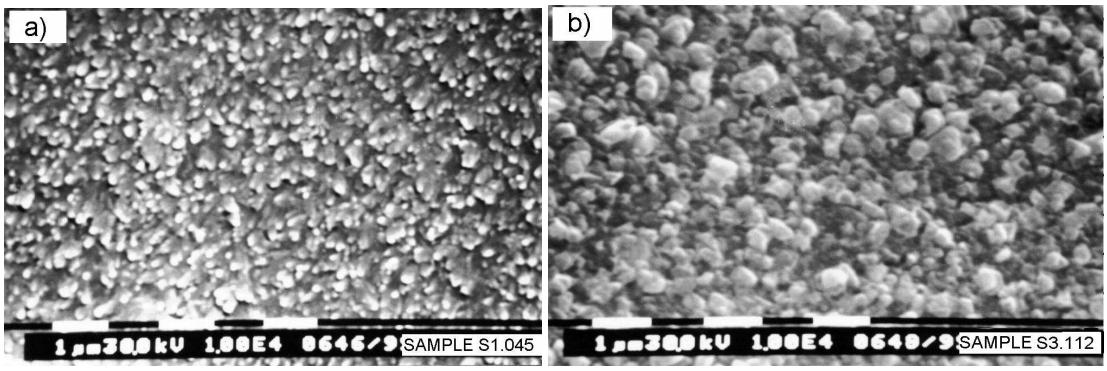

Fig. 2. Scanning electron micrographs of Sb_2S_3 thin films: (a) d=0.45 μm (b) d=1.12 μm.

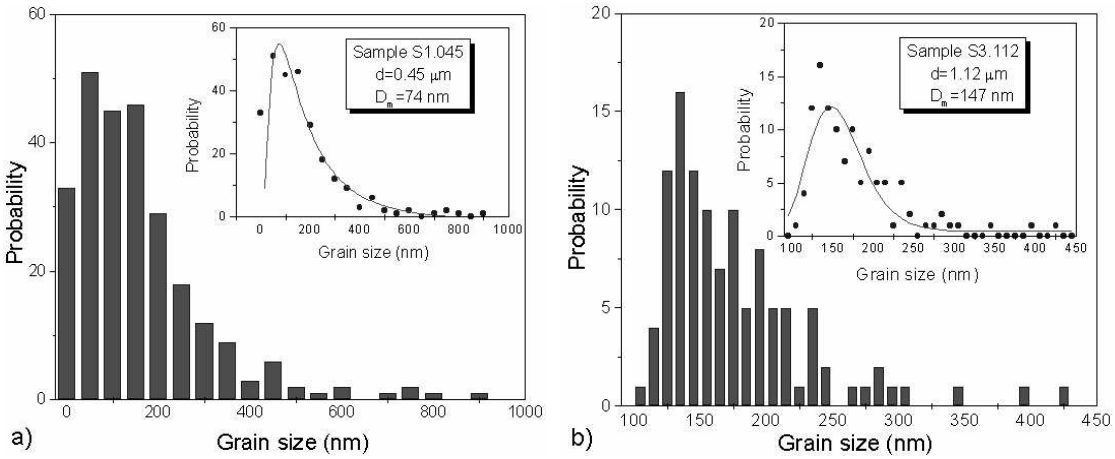

Fig. 3. Grain size distribution of the Sb_2S_3 thin films: (a) d=0.45 μm, (b) d=1.12 μm.

The study of the temperature dependence of the electrical conductivity during the heat treatment may provide valuable information on the processes tacking place in the films. In this connection, the shapes of the $\ln\sigma = f(10^3/T)$ curves were examined. Experimentally, it was established that the samples with stable structure and reproducible electronic transport can be obtained if, after deposition, the respective samples are submitted to a heat treatment, consisting of

several heating/cooling cycles (temperature rate was about 5 K/min) within a temperature range 287-447 K. The shape of the temperature dependences of the electrical conductivity during heat treatment depends on the film thickness and preparation conditions. However, some similar behaviour aspects were observed for all investigated samples.

Typical $ln\sigma = f(10^3 / T)$ curve during heat treatment is illustrated in Fig. 4(a) for one of studied sample. The respective sample was subjected to two successive heating and cooling cycles in the temperature range 287-447 K. An exponential increase of σ with temperature has been observed in all temperature range. We suppose that the well-known exponential law can describe the temperature dependence of the electrical conductivity [34,35]

$$\sigma = \sigma_0 \, exp\left(-\frac{E_a}{k_B T}\right) \tag{3}$$

where σ_0 is a parameter depending on the sample characteristics (thickness, structure, etc.), E_a denotes the thermal activation energy of electrical conduction, and k_B is Boltzmann's constant.

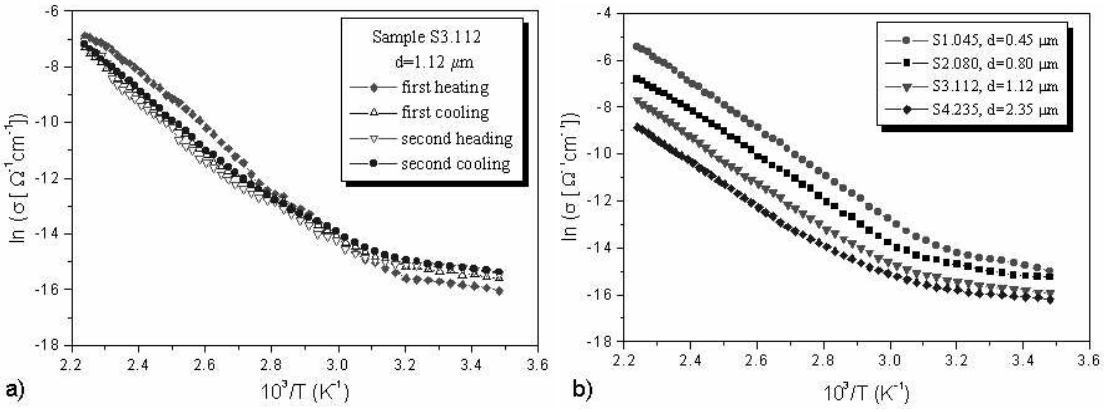

Fig. 4. (a) Temperature dependence of the electrical conductivity during heat treatment; (b) Temperature dependence of the electrical conductivity for heat-treated samples.

The conduction mechanism in investigated samples can be explained by applying the models elaborated for the films with polycrystalline structure [27,36]. We consider that the Seto's model [23,24] with several modifications proposed by Baccarani et al. [25,26] could explain the mechanism of electron transfer in investigated Sb_2S_3 thin films.

The following assumptions were made in this model: (a) the crystallites have similar size and shape, ℓ; (b) only one type of singlevalent trapping states (having concentration N_t and energy E_t with respect to Fermi level at the interface E_i) is uniformly distributed within crystallites; (c) the traps are initially neutral and become charged by trapping a free carrier; (d) the crystallite boundary thickness is negligible with respect to crystallite size; (e) the crystallites are n-type semiconductors and donor concentration is N_D.

According to this model, for a given set of ℓ, N_t and E_t there is an impurity concentration N_D^* such that, if $N_D^* > N_D$ the crystallites are partially depleted and the expression of electrical conductivity can be determined for the following energy domains [25]:

1) For energy domain: $E_F - E_t - E_b >> k_B T$, electrical conductivity of films can be described by the expression:

$$\sigma = \frac{e^2 \, \ell \, N_C^2 \, \nu \, n_0}{k_B T} \, exp\left(-\frac{E_a}{k_B T}\right) \tag{4}$$

where

$$\nu = \left(\frac{k_B T}{2\pi m^*}\right)^{1/2} \tag{5}$$

and the activation energy, E_a, is equal whith the energy barrier at crystallite boundary, E_b, given by expression

$$E_b = \frac{e^2 \ell^2 N_D}{8\varepsilon_r} \tag{6}$$

2) For energy domain $E_t + E_b - E_F >> k_B T$, the electrical conductivity of films can be written as

$$\sigma = e N_C^2 \nu (2\varepsilon_r N_D^{-1} E_b)^{1/2} (k_B T N_t)^{-1} exp\left(-\frac{E_a}{k_B T}\right) \tag{7}$$

and the activation energy, E_a, is given by

$$E_a = \frac{E_g}{2} - E_t \tag{8}$$

where E_g is energy bandgap of Sb_2S_3 thin films.

In the Eqs. (4)-(7) the following notations have been used: e, electron charge; N_C, effective state density for the conduction band; T, absolute temperature; m^*, scalar effective mass of charge carriers; ε_r, low-frequency dielectric constant of crystallites; n_0, electron concentration in neutral region of crystallites and E_F, Fermi energy.

It can be observed from Fig. 4(b) that, the $ln\sigma = f(10^3 / T)$ curves for heat-treated samples exhibit two linear regions. The first, in the lower temperature range 287-320 K is characterized by smaller slope. By assuming that in this temperature range, the expression (4) is valid, from the slopes of $ln\sigma = f(10^3 / T)$ curves, the values of the energy barrier, E_b, have been calculated for respective samples (Table 1). In the higher temperature range 320-447 K, larger slopes characterize the curves. In this region the E_a values are close to $E_g/2$. The values of energy bandgap, E_g, of Sb_2S_3 thin films were determined from optical measurements [21,22]. The values of energy of the trapping states, E_t, have been calculated by taking into account the equation (8). These values are listed in Table 1.

Table 1. Electronic parameters of some investigated Sb_2S_3 thin films.

Sample	d (μm)	ℓ (nm)	E_b (eV)	E_a (eV)	E_g (eV)	E_t (eV)	N_D (cm^{-3})	N_t (cm^{-3})
S1.045	0.45	74	0.232	0.860	2.417	0.348	1.26×10^{17}	1.34×10^{13}
S2.080	0.80	86	0.156	0.833	1.817	0.048	1.13×10^{17}	1.25×10^{13}
S3.112	1.12	147	0.141	0.758	1.527	0.005	0.76×10^{17}	1.62×10^{13}
S4.235	2.35	152	0.123	0.701	1.412	0.005	0.32×10^{17}	0.88×10^{13}

The impurity concentrations N_D, have been calculated from the equation (6). The crystallite size was determined by means SEM micrographs and the low-frequency dielectric constant was considered to be ε_r=13.6 for crystalline Sb_2S_3 [4,37]. By substituting the N_D values and σ values (estimated at 400 K from $ln\sigma = f(10^3 / T)$ curves) into Eq. (7), the values of the N_t were calculated. The obtained values for N_D and N_t are indicated in Table 1.

Generally, the heating of Sb_2S_3 thin films affects its structural characteristic and consequently, the transport properties of films could be changed. We suggest that the mechanism of the electrical conduction in studied samples is influenced by inter-crystallite boundaries, characterized by high resistivity [36]. From SEM micrographs it can be observed that the heat treatment determines an increases in the crystallite size, and the thickness of the films increases. In these conditions the inter-crystallite domains increases and consequently, the electrical conductivity of the films decreases. For the investigated samples, the thermal activation energy of electrical conduction, E_b, varied from 0.123 eV to 0.232 eV for the first part of the curves $ln\sigma = f(10^3 / T)$ (Fig. 4) and between 0.701 eV to 0.860 eV for next part, (E_a in Table 1).

4. Conclusions

Sb_2S_3 thin films were prepared using the vacuum evaporation technique. Structural investigation shows that as-deposited films exhibit an amorphous structure.

In order to obtain films with stable structure and reproducible properties all films were subjected to a heat treatment consisting of two successive heating/cooling cycles. After heat treatment the films become polycrystalline. The obtained results related to the temperature dependence of the electrical conductivity are interpreted in terms of Seto's model proposed for polycrystalline semiconducting films. The impurity concentration and the density of the trapping states at the grain boundary have been calculated for investigated samples. The inter-crystallite boundaries of thin films play an important role in the mechanism of electrical conduction.

References

[1] J. Grigas, J. Meshkanskas, J. Orlimans, Physica Status Solidi **(A)37**, 10 (1976).
[2] M. S. Ablova, A. A. Andreev, T. T. Degegkaev, B. T. Melekh, A. B. Pevtsov, N. S. Shendel, L. N. Shurnilova, Sov. Phys. Semicond. **10**, 6 (1976).
[3] M. J. Chokalingam, K. Nagaraja Rao, R. Rangarajan and C. V. Suryanarayana, J. Phys. D.: Appl. Phys. **3**, 1641 (1970).
[4] G. Ghosh, B. P. Varma, Thin Solid Films **69**, 61 (1979).
[5] E. Montrimass, A. Pazera, Thin Solid Films **34**, 65 (1976).
[6] J. George and M. K. Radhakrishan, Solid State Commun. **33**, 987 (1980).
[7] M. T. S.Nair, Y. Pena, J. Campos, V. M. Garcia, P. K. Nair, J. Electrochem. Soc. **145**, 2113 (1998).
[8] S. M. Sze, Physics of Semiconductor Devices, Wiley, New York (1981).
[9] R. S. Mane, B. R. Sankapal, C. D. Lokhande, Thin Solid Films **353**, 29 (1999).
[10] J. D. Desai, D. D. Lokhande, Thin solid Films **237**, 29 (1994).
[11] O. Savadogo, K. C. Manda, Solar Energy Mater. Solar Cell **26**, 117 (1992).
[12] C. H. Bhosale, M. D. Uplane, P. S. Patil, C. D. Lokhande, Thin Solid Films **248**, 137 (1994).
[13] V. V. Killedar, C. D. Lokhande, C. H. Bhosale, Mater. Chem. Phys. **47**, 104 (1997).
[14] S. Mahanty, J. M. Merino, M. Leon, J. Vac. Sci. Technol. **A15**, 3060 (1997).
[15] P. Arun, A. G. Vedeshwar, J. Non-Cryst. Solids **220**, 63 (1997).
[16] I. K. El Zawawi, A. Abdel-Moez, F. S. Terra, M. Mounir, Thin Solid Films **324**, 300 (1998).
[17] I. K. El Zawawi, A. Abdel-Moez, F. S. Terra, M. Mounir, Fizika **A7**(3), 97 (1998).
[18] A. G. Vedeshwar, J. Phys. III France **5**, 1161 (1995).
[19] A. M. Salem, M. Soliman Selim, J. Phys.D: Appl. Phys. **34**, 12 (2001).
[20] V. D. Das, L. Damodure, J. Appl. Phy. **81**, 1522 (1997).
[21] N. Tigau, G. I. Rusu, C. Gheorghies, J. Optoelectron. Adv. Mater. **4**, 943 (2002)
[22] N. Tigau, V. Ciupina, G. Prodan, G. I. Rusu, C. Gheorghies, E. Vasile, J. Optoelectron. Adv. Mater. **1**, 211 (2004).
[23] J. Y. W. Seto, J. Electrochem. Soc. **122**, 701 (1975).
[24] J. Y. W. Seto, J. Appl. Phys. **465**, 247 (1975).
[25] G. Baccarani, B. Rico, G. Spandini, J. Appl. Phys. **49**, 5565 (1978).
[26] C. H. Seager, T. G. Gastner, J. Appl. Phys. **49**, 3879 (1978).
[27] K. L. Chopra, Thin Film Phenomena, McGraw-Hill, New York, (1969).
[28] G. I. Rusu, I. Caplanus, L. Leontie, A. Airinei, D. Mardare, I. I. Rusu, Acta Mater. **49**, 553 (2001).
[29] M. S. Droichi, F. Vaillant, E. Bustarret, D. Jousse, J. Non-Cryst. Solids **101**, 151 (1997).
[30] K. Y. Rajpure, A. L. Dhebe, C. D. Lokhande, C. H. Bhosale, Mater. Chem. Phys. **56**, 177 (1998).
[31] Y. Wada, S. Nishimatsu, J. Electrochem. Soc. **125**, 1499 (1978).
[32] J. E. Palmer, C. V. Thompson, H. I. Smith, J. Appl. Phys. **62**, 2492 (1987).
[33] R. A. Ristau, K. Barmak, K. R. Coffey, J. K. Howard, J. Mater. Res. **14**, 3263 (1999).
[34] H. F. Wolf, Semiconductors, Wiley, New York, 1971.
[35] K. Seeger, Semiconductors Physics, Springer, Berlin, 1999.
[36] L. L. Kazmerski (ed.), Polycrystalline and Amorphous Thin Films and Devices, Academic Press, New York, 1980.
[37] B. H. Juarez, S. Rubio, J. Sanchez-Dehesa, C. Lopez, Adv. Mater. **20**, 1486 (2002).